



Precipitation Extremes and Water Vapor

Relationships in Current Climate and Implications for Climate Change

J. David Neelin¹ · Cristian Martinez-Villalobos^{2,3} · Samuel N. Stechmann⁴ · Fiaz Ahmed¹ · Gang Chen¹ · Jesse M. Norris¹ · Yi-Hung Kuo¹ · Geert Lenderink⁵

Accepted: 15 November 2021 / Published online: 5 February 2022
© The Author(s) 2022

Abstract

Purpose of Review: Review our current understanding of how precipitation is related to its thermodynamic environment, i.e., the water vapor and temperature in the surroundings, and implications for changes in extremes in a warmer climate.

Recent Findings: Multiple research threads have i) sought empirical relationships that govern onset of strong convective precipitation, or that might identify how precipitation extremes scale with changes in temperature; ii) examined how such extremes change with water vapor in global and regional climate models under warming scenarios; iii) identified fundamental processes that set the characteristic shapes of precipitation distributions.

Summary: While water vapor increases tend to be governed by the Clausius-Clapeyron relationship to temperature, precipitation extreme changes are more complex and can increase more rapidly, particularly in the tropics. Progress may be aided by bringing separate research threads together and by casting theory in terms of a full explanation of the precipitation probability distribution.

Keywords Rainfall · Climate change · Deep convection · Extreme events · Precipitation probability · Stochastic model

Introduction

Examination of climate change impacts on the probability of strong precipitation events has been an ongoing effort since the late 1980s (Noda and Tokioka 1989) and much work since then (e.g., Meehl et al. 2000; Allen and

Ingram 2002; Trenberth et al. 2003; Tebaldi et al. 2006; Min et al. 2011; Chou et al. 2012; O’Gorman 2012; Wuebbles et al. 2014; Sillmann et al. 2013; Pendergrass and Hartmann 2014; Myhre et al. 2019; Papalexiou and Montanari 2019; Tabari 2020) including reviews by Schneider et al. (2010), Trenberth (2011), O’Gorman (2015) and Donat et al. (2020). However, confidence in projections of precipitation change is affected by limitations in simulations of various aspects of precipitation in current climate (e.g., Biasutti et al. 2006; Qian et al. 2015; Lintner et al. 2017; Hagos et al. 2021; Biasutti et al. 2018), by differences in the projection of changes in extreme precipitation among models, especially in the tropics (Pendergrass et al. 2019), by sensitivity to model parameters (e.g., Knight et al. 2007; Sanderson 2011; Covey et al. 2013; Bernstein and Neelin 2016; Qian et al. 2018), and by limited understanding of the interaction between the large-scale flow and small-scale convective precipitation (Tomassini 2020). Narrowing uncertainties in simulated precipitation probability distribution changes becomes all the more important as procedures for event attribution (Haustein et al. 2016; Eden et al. 2016; van der Wiel et al. 2017; van Oldenborgh et al. 2017; Emanuel

This belongs to Topical Collection on *Precipitation Extremes and Climate Change*

✉ J. David Neelin
neelin@atmos.ucla.edu

¹ Department of Atmospheric and Oceanic Sciences, University of California, Los Angeles, CA, 90095-1565, USA

² Faculty of Engineering and Science, Universidad Adolfo Ibáñez, Peñalolén, Santiago, Chile

³ Data Observatory Foundation, Santiago, Chile

⁴ Department of Mathematics and Department of Atmospheric and Oceanic Sciences, University of Wisconsin—Madison, Madison, WI, USA

⁵ Royal Netherlands Meteorological Institute, De Bilt, Netherlands

2017; Risser and Wehner 2017; Pall et al. 2017; Wang et al. 2018) potentially inform decisions regarding whether and how to rebuild after extreme events. Such procedures provide estimates of the extent to which probabilities of equaling or exceeding a given event size have changed due to anthropogenic warming, typically using ensembles of current climate simulations compared to simulations approximating conditions that would have occurred in absence of anthropogenic emissions.

It has been common to ask whether precipitation scales with the Clausius-Clapeyron (CC) relationship of saturation water vapor to temperature, roughly 7% per degree Celsius of large-scale warming or whether it increases slower (Eden et al. 2016), or faster than this, the latter termed “super-CC” scaling (Pall et al. 2007; Lenderink and Van Meijgaard 2008; Sugiyama et al. 2010; Loriaux et al. 2013; Prein et al. 2017; Wasko and Sharma 2014; Lenderink et al. 2017; Pfahl et al. 2017; Pendergrass 2018). Various simple balances based on approximations to the moisture budget or energy balance, respectively, have been put forward, as discussed in the Section “Moisture Equation and Thermodynamic Equation”, but these do not attempt to explain the underlying distributions of precipitation or vertical velocity. Diagnostic statements based on these budgets often divide changes in moisture convergence into those associated with changes in moisture, commonly termed the “thermodynamic” contribution, and those associate with changes in convergence, termed the “dynamic” contribution, with the latter being viewed as separate and not easily explained.

At the same time, there have been advances in understanding the relationship of precipitation—particularly that associated with deep convection—to its temperature and moisture environment. Part of this literature has shown that essential features of the precipitation distribution can be explained relatively simply in terms of the onset of precipitation in relationship to variations affecting this thermodynamic environment. These results imply that the thermodynamic and dynamic contributions affect the precipitation jointly. Indeed, for the tropical case, we argue that the thermodynamic and dynamic components are involved in a feedback such that it may be more productive for the field to move away from this artificial separation.

Key Balances

Moisture Equation and Thermodynamic Equation

The vertically integrated moisture equation may be written:

$$\langle \partial_t q \rangle + \langle \nabla \cdot \mathbf{v}q \rangle = E - P, \quad (1a)$$

where q is water vapor mixing ratio, t is time, P is precipitation, E is evaporation, \mathbf{v} is the horizontal wind

vector and $\langle x \rangle = \int_0^{p_s} x dp/g$ denotes a mass weighted integral in pressure coordinates, with p_s surface pressure, and g the gravitational acceleration. Equivalently, (1a) can be written as

$$\langle \partial_t q \rangle + \langle \mathbf{v} \cdot \nabla q \rangle + \langle \omega \partial_p q \rangle = E - P, \quad (1b)$$

where the transport term has been rewritten using $\langle \nabla \cdot \mathbf{v}q \rangle = \langle \mathbf{v} \cdot \nabla q \rangle + \langle \omega \partial_p q \rangle$, where ω is vertical pressure velocity, with the vertical transport term being equivalent to the moisture integrated with the horizontal convergence.

Similarly, the vertically integrated thermodynamic energy equation (temperature equation) is, in an approximation sufficient for present purposes,

$$\langle \partial_t c_p T \rangle + \langle \mathbf{v} \cdot \nabla c_p T \rangle + \langle \omega \partial_p s \rangle = \langle Q_c \rangle + F_s \quad (2)$$

with T the temperature, $s = c_p T + \phi$ the dry static energy, c_p the heat capacity at constant pressure, ϕ the geopotential, F_s the net flux of longwave and shortwave radiation plus sensible heat into the column. The convective heating Q_c includes latent heat release by condensation and freezing processes and vertical transport by subgrid scale convective motions, and can here be approximated as $\langle Q_c \rangle = LP$, with L the net latent heat of condensation released per unit of moisture loss by precipitation. Condensate loss to the column by lateral transport is sometimes represented by a precipitation efficiency (Muller and Takayabu 2020), which is particularly relevant at smaller scales or high rates of moisture convergence, and ideally should be modeled by including a condensate equation. Freezing processes are not explicitly addressed here for brevity, but can be included using a frozen moist static energy (Wing et al. 2007, 2014).

The leading balance for the moisture equation under heavily precipitating conditions, especially in the tropics, can be written equivalently as either

$$\langle qC \rangle \approx P \quad \text{or} \quad -\langle \omega \partial_p q \rangle \approx P \quad (3)$$

defining convergence $C = -\nabla \cdot \mathbf{v}$, and using the continuity equation $C = \partial_p \omega$, assuming that ω is small at upper and lower limits of integration. With moisture being relatively small in the upper troposphere these approximately correspond to a balance between low-level moisture convergence and precipitation. Likewise, the leading balance for the thermodynamic equation under similar circumstances can be written equivalently as either

$$-\langle sC \rangle \approx LP \quad \text{or} \quad \langle \omega \partial_p s \rangle \approx LP. \quad (4)$$

We note that for the climatology, evaporation and energy fluxes cannot be neglected because the leading order balances (3)–(4) disappear in the vertically integrated moist static energy equation due to the cancellation between the moisture sink and the convective heating associated with precipitation. Likewise, for the evolution of storm systems, terms that would be apparently small in moisture

and thermodynamic equations separately, including the time derivative of moisture, can be important. In the midlatitudes where horizontal advection is important, (4) may be refined with the quasi-geostrophic omega equation (O’Gorman 2015; Nie et al. 2018) which includes the effects of vorticity and temperature advection on vertical velocity. It is further worth underlining that a dominant source of variations leading to the probability density function (pdf) of precipitation arises from the variations in convergence.

“Thermodynamic” and Dynamical Contributions and Issues

For changes in mean precipitation, defining Δx to be the difference in time mean under a global warming scenario relative to historical climatology, denoted with \bar{x} , it has been common to diagnose the changes in the moisture budget as:

$$\langle \Delta q \bar{C} \rangle + \langle \bar{q} \Delta C \rangle + \dots = \Delta P - \Delta E \quad (5)$$

where “...” denotes additional terms such as changes in $\mathbf{v} \cdot \nabla q$ and transients (e.g., Seager et al. 2014), and the second-order covariance term $\langle \Delta q \Delta C \rangle$ is ignored. The first and second terms in (5) have come to be referred to as the “thermodynamic” and “dynamic” contributions, respectively (Chou and Neelin 2004; Emori and Brown 2005; Held and Soden 2006; Oueslati et al. 2019; O’Gorman et al. 2021), where the thermodynamic terminology for related analysis of clouds (Bony et al. 2004) quickly supplanted “direct moisture effect” (Chou and Neelin 2004). This breakdown between the two components highlights that the rich-get-richer or wet-get-wetter effect (i.e., regions where historically precipitation exceeds evaporation will receive enhanced precipitation, while regions where historically evaporation exceeds precipitation will become even drier) arises from the thermodynamic term, but can be regionally increased or offset by the dynamic term.

A corresponding division can be defined for precipitation quantiles (Emori and Brown 2005; Chen et al. 2019; Norris et al. 2019a), with x_i denoting x conditioned on the i^{th} quantile of P in historical or future climatology and Δx_i denoting the change of x at the i^{th} quantile of P in a warmer climate. We use percentiles or return time in the historical climatology to refer to these quantiles where convenient. The leading balances for precipitation P_i at a given quantile are

$$\langle \Delta q_i C_i \rangle + \langle q_i \Delta C_i \rangle \approx \Delta P_i \quad (6)$$

with the first and second terms on the LHS again termed thermodynamic and dynamic. The first term represents additional moisture in a warmer climate subject to the present-day circulation when precipitation extremes occur, while the second term represents the future changes to circulation when extremes occur acting on present-day

moisture. However, each grid point is typically analyzed in isolation (Emori and Brown 2005; Pfahl et al. 2017; Tandon et al. 2018; Norris et al. 2019a), so that, unlike for the mean budget (5), C_i does not represent a closed circulation.

The thermodynamic term, $\langle \Delta q_i C_i \rangle$, is well predicted by the increase in temperature corresponding to the given quantile of P , with about 7% increase of moisture at each vertical level per K warming, as per the Clausius-Clapeyron relation (Chen et al. 2019; Norris et al. 2019a). The dynamic term, $\langle q_i \Delta C_i \rangle$, could in theory result from an amplification/dampening of the circulation or a change in the vertical structure of the circulation. In the CESM Large Ensemble, the component relating to vertical structure is small, so that the dynamic term approximately results from a rescaling of the circulation when precipitation occurs (Chen et al. 2019; Norris et al. 2019a).

For precipitation event accumulations, i.e., precipitation integrated from beginning to end of a rain event, a similar budget can be written that also involves duration, although changes in the latter tend not to be of leading importance (Norris et al. 2019b) in diagnostics of the Community Earth System Model (CESM) Large Ensemble.

This approximation neglects the conditionally averaged terms such as $\langle \partial_t q \rangle_i$, which is small in the tropics and shows some cancellation with $\langle \mathbf{v} \cdot \nabla q \rangle_i$ for midlatitude weather systems (Chen et al. 2019; Norris et al. 2019a). In other words, extreme precipitation is maintained not by the water vapor being reduced in the column but by moisture transport. The covariance between q_i and C_i at each percentile is also ignored (i.e., $\langle q C \rangle_i \approx \langle q_i C_i \rangle$), with the vertical structure of C_i varying with percentile.

Figure 1 shows an example of this decomposition for changes in 10-year event accumulation size between 1990–2005 and 2071–2080 from the CESM large ensemble under the scenario for anthropogenic emissions Representative Concentration Pathway RCP8.5 (Meinshausen et al. 2011). While the contribution from moisture changes is substantial both within and outside the tropics, the enhancement by convergence changes is particularly large in certain regions of the tropics. At longer return times (not shown), both contributions are larger, and the dynamical contribution tends to be further enhanced (Norris et al. 2019b). Similar spatial structures of thermodynamic and dynamic components, conditioned on precipitation extremes, have been calculated by other methods (Emori and Brown 2005; Held and Soden 2006; Pfahl et al. 2017; Tandon et al. 2018). In midlatitude regions where precipitating events are often associated with Atmospheric Rivers (ARs) (Zhu and Newell 1998; Gimeno et al. 2014; Waliser and Guan 2017; Ralph et al. 2017; Valenzuela and Garreaud 2019), projected changes to ARs likewise depend on changes to convergence as well as changes in moisture (Ma et al. 2019; Payne et al. 2020).

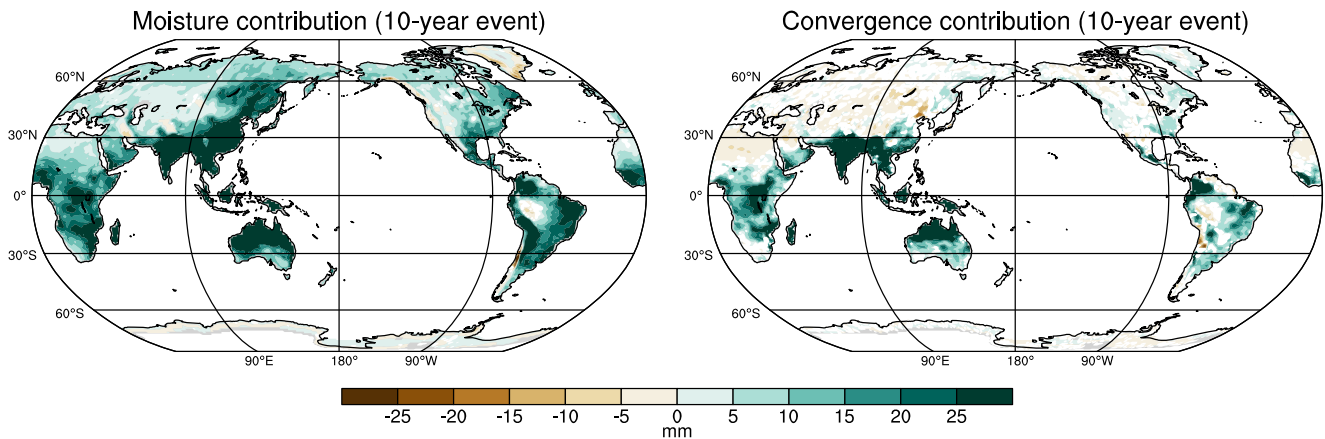


Fig. 1 Contributions to changes in 10-year event accumulation size (mm) over global land due to changes in moisture and in convergence, respectively, a.k.a. thermodynamic and dynamic contributions from the CESM large ensemble between 1990–2005 and 2071–2080

A closely related diagnostic of the dynamic and thermodynamic contributions has been advocated based on approximations to the energy budget. If the stratification ($-\partial_p s$) is assumed to be approximately moist adiabatic in convective regions, it can roughly be replaced by $\partial_p q_{sat}$ in (4) (Muller et al. 2011; Muller and Takayabu 2020) with the saturation specific humidity q_{sat} evaluated along moist adiabats. Given that departures from moist adiabatic structure are noted in observations even in heavily precipitating conditions (Holloway and Neelin 2009, 2010; Schiro et al. 2016), one might ask what the role is for this approximation compared to simply using the moisture equation leading balance (3) (e.g., Chou et al. 2012). Indeed, for some purposes the two formulations behave similarly (Muller and Takayabu 2020). Two useful aspects of making this approximation are that (i) the dry stability ($-\partial_p s$) tends to vary less than the moisture in the large-scale convective environment, and (ii) it provides an indication of how the stratification may be expected to change with warming, partially compensating increases in moisture, without having to assume constant relative humidity. However, it is worth underlining that the overall stability for moist motions also depends on the vertical structure and vertical extent of the vertical velocity in (4), both of which may change.

If we expand (4) for quantiles, an expression parallel to (6)—and with similar approximations—for the thermodynamic equation is:

$$-\langle \Delta s_i C_i \rangle - \langle s_i \Delta C_i \rangle \approx L \Delta P_i \quad (7)$$

For midlatitudes, this thermodynamic balance may be combined with vorticity and temperature advection in the quasi-geostrophic omega equation which can give similar dynamic amplification from increases in convective heating (Nie et al. 2018) with competition among changes in

under RCP8.5, adapted from (Norris et al. 2019b). Note the substantial enhancement by convergence changes in certain regions in the tropics. Missing values are where fewer than 80% of bootstrap replications agree on the sign of the change

moisture, dry stratification in depth of heating (Li and O’Gorman 2020) and nonlinearity of the heating response (Nie et al. 2020). While the thermodynamic budget (7) has not yet been quantified in the same ways as (6), it allows us to make a simple but important point. Combining (6)–(7) to eliminate P yields a balance governing the dynamical changes

$$\langle (s_i + Lq_i) \Delta C_i \rangle \approx -\langle (\Delta s_i + L \Delta q_i) C_i \rangle + \dots \quad (8)$$

where “+...” is a reminder that terms considered small relative to P in (6) and (7) are not necessarily negligible here. The terms in Δq_i and Δs_i on the rhs of (8) must be balanced by the ΔC_i term on the lhs. In other words, the interaction of the thermodynamic equation with the moisture equation can imply that changes in the dynamical terms must arise, i.e., there can be a *thermodynamic requirement that changes in convergence occur*. The substantial dynamical feedback at long return times in the tropics, or under midlatitude convective conditions where these balances apply, should thus be expected as seen in Fig. 1. In this sense, the term “thermodynamic” for changes associated only with moisture is a misnomer, and the division between thermodynamic and dynamic effects is artificial. We hypothesize that progress in better understanding intense precipitation changes, especially in the tropics, will require theory that combines both of these effects, especially since both combine naturally in the theory of how precipitation probability distributions arise, outlined in the Section “[How Precipitation Distributions Arise: Variations Across a Moisture/Buoyancy Threshold](#)”.

Scaling Arguments

There are variants in the way the term “scaling” is used for precipitation, but in essence they posit that the precipitation

probability distribution, or some aspect of it, under the warmer climate is similar to that under historical conditions once precipitation is scaled by some factor. This can be argued from leading balances in either the moisture (3) (Pall et al. 2007; O’Gorman and Schneider 2009, 2009; Trenberth 2011; Chou et al. 2012) or thermodynamic (4) (Muller et al. 2011), assuming that the short timescale variations that lead to the distribution come primarily from convergence and change little in the warmer climate, while the large-scale moisture or stratification increases by a factor $(1 + \gamma)$, with γ given by Clausius-Clapeyron. Chou et al. (2012) posit that the pdf $prob(P)$ of a given precipitation intensity P would thus simply be $prob(P/(1 + \gamma))$ under the warmer climate, formalizing the assumption that the precipitation axis simply rescales. Pendergrass and Hartmann (2014) rephrase this as a “shift mode” since rescaling the precipitation by a constant factor is equivalent to a shift in log-precipitation. In the Section “How Precipitation Distributions Change: Changes in Extremes”, it becomes clear why this holds well for event accumulations but imperfectly for daily average intensities.

A number of studies have sought ways to examine such scaling in current climate (Lenderink and Van Meijgaard 2008, 2015, 2019; Wasko and Sharma 2015; Westra et al. 2014). Figure 2 combines examples from two such studies that typify key points from this endeavor. A measure of extreme precipitation, such as a high percentile, is binned by dew point temperature (typically near-surface values are used) across a range of conditions in current climate. Dew point temperature is a measure of water vapor or absolute humidity of the air. Since much of the atmospheric water vapor resides in the atmospheric boundary layer, near-surface dew point temperature is related to the column water vapor (CWV) and, likewise, near-surface humidity is also a measure of the potential for latent heating in a simple updraft parcel framework, and therefore a proxy for one contribution to buoyancy (see the Section “Precipitation Relationship to the Thermodynamic Environment”). If the near-surface dew point temperature could be taken to be typical conditions through the lower tropospheric layer that contributes to moisture convergence in storms, then the scaling of precipitation extremes as a function of this by 7% per C could be said to be CC and more rapid changes super-CC. The green curve in Fig. 2 exemplifies a number of observational studies that find changes that are faster than CC in this sense. While the interpretation of scaling is complex and some confounding factors may also explain super-CC behavior (Haerter and Berg 2009; Zhang et al. 2017; Lenderink et al. 2018), dynamical feedbacks in convective rain systems that enhance moisture convergence ($\langle q_i \Delta C_i \rangle$) are usually considered to play a key role in explaining super-CC scaling (Loriaux et al. 2013; Berg et al. 2013; Lenderink et al. 2017; Lochbihler et al. 2017; Haerter and Schlemmer 2018; Lochbihler et al. 2021).

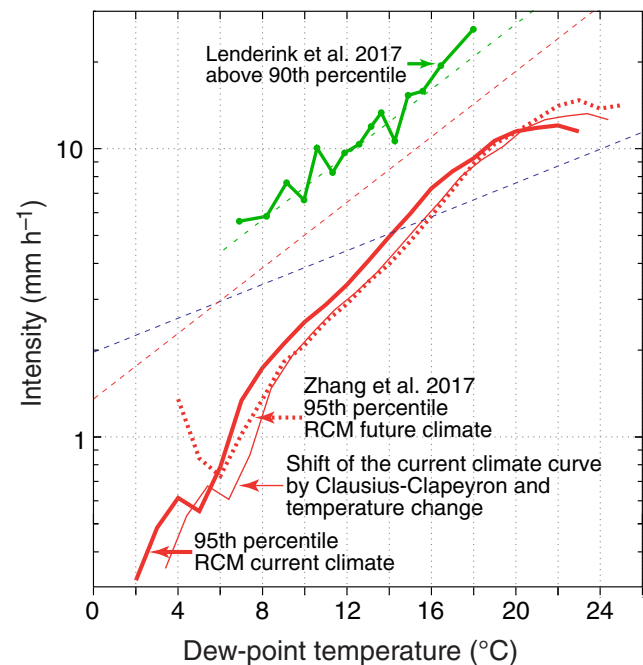


Fig. 2 Measures of precipitation intensity (log scale) as a function of dew point temperature. Green curve: observed hourly event peak precipitation intensities above the 90th percentile from summertime afternoon and evening events from stations in the Netherlands (adapted from Lenderink et al. 2017), with dashed line indicating 2CC scaling ($14\% \text{ C}^{-1}$) for reference. Red solid and dashed curves: 95th percentile hourly precipitation intensity from current and future climate simulations, respectively, with the Rossby Center regional climate model over the Netherlands, with thin red curve showing CC-based prediction, shifting the current climate curve by the projected warming and multiplying by 1.07 (adapted from Zhang et al. 2017)

Another step in this argument is whether the variations in meteorological conditions that lead to these diagrams in current climate can potentially be interpreted as characterizing the way they will scale with temperature under global warming (Fowler et al. 2021). An analysis of this by Zhang et al. (Zhang et al. 2017) is summarized by the red curves in Fig. 2. A hydrostatic regional climate model reproduces apparent super-CC scaling in current climate, but under a greenhouse change scenario, the change of the curve does not follow the current climate curve, but rather the curve shifts in a manner that is more consistent with CC. A similar result was earlier obtained (Sahany et al. 2014) for the way that curves characterizing the onset of convection shift under warming.

Despite these caveats, there is considerable evidence in model simulations for regions of super-CC scaling (Attema et al. 2014; Lenderink et al. 2019; Singleton and Toumi 2013; Prein et al. 2017; Lochbihler et al. 2019). Also, convection-permitting climate model simulations reveal shifts in scaling curves exceeding the CC rate, in particular for the most extreme events and for scenarios that have

relatively small lapse rate changes (Lenderink et al. 2021). Maps of fractional change in precipitation at a given high percentile in model simulations of global warming provide one means of visualizing the scaling as a function of region. Commonly there are some super-CC regions, i.e., where this fractional change is larger than expected from CC scaling, especially within the tropics (Pall et al. 2007; Sugiyama et al. 2010; Hoegh-Guldberg et al. 2018), as further discussed in the Section “How Precipitation Distributions Change: Changes in Extremes”. Indications of a band of super-CC scaling within the tropics may also be seen in observed annual maximum precipitation (Westra et al. 2013), although highly uneven spatial coverage places caveats on this.

The key balances of the Section “Thermodynamic” and Dynamical Contributions and Issues” suggest a reason for this. The thermodynamic contribution tends to obey CC scaling, so departures from this tend to occur where the dynamical contribution is substantial. The moist static energy balance (8) suggests that there are conditions under which this must occur, and furthermore be proportional to changes in moisture and stratification. If we approximate $\langle s_i \Delta C_i \rangle \approx -M_{si} \Delta C_i^*$, $\langle Lq_i \Delta C_i \rangle \approx M_{qi} \Delta C_i^*$, with ΔC_i^* characterizing the low-level convergence and the change in vertical structure being small, (6)–(7) yield

$$\Delta P_i \approx \underbrace{\langle \Delta q_i C_i \rangle}_{\text{“thermodynamic”}} + \underbrace{\langle (\Delta s_i L^{-1} + \Delta q_i) C_i \rangle (M_{qi} / M_i)}_{\text{dynamic required by thermodynamics}} \quad (9)$$

with M_{qi} a gross moisture stratification for the changes, and $M_i = M_{si} - M_{qi}$ a gross moist stability (which is typically smaller). The first term is the effect commonly termed “thermodynamic”, which yields CC scaling if Δq_i changes with constant relative humidity. The second term represents the result of the feedback between convective heating and convergence changes required by simultaneously satisfying thermodynamic and moisture balances. Recall that it is commonly termed “dynamic” because it entails changes in the flow; the form here clarifies that the vertical velocity changes are proportional to moisture and stability changes that initiate the feedback. It tends to amplify the precipitation changes if the moisture change effect in the feedback term is larger than the compensation by stratification increases, and thus tends to yield changes that differ from CC scaling. The importance of feedbacks from changes in convective heating on changes in vertical motion have been noted in multiple studies (Pall et al. 2007; Pendergrass and Gerber 2016; Lenderink et al. 2017; Berg et al. 2013; Singleton and Toumi 2013; Nie et al. 2018) to varying degrees (Abbott et al. 2020). We underline that (9) is a statement of this, phrased in terms of the large-scale moist stability of the thermodynamic environment. There have been slow advances in theory and diagnostics of gross moist stability over the years (Neelin and Held 1987, 2000, 2007; Yu

et al. 1998; Back and Bretherton 2006; Raymond et al. 2007; Raymond et al. 2009; Muller and O’Gorman 2011; Inoue and Back 2015, 2017), but (9) suggests a need for further advances. It makes the basic point that super-CC scaling of changes is quite reasonable to expect under conditions that can be widespread in the tropics.

Precipitation Relationship to the Thermodynamic Environment

A more quantitative route to modeling and understanding precipitation extremes must relate precipitation to its thermodynamic environment, in a manner more similar to a parameterization of precipitation. An empirical relationship linking tropical oceanic precipitation to its environmental moisture content has been noted at both daily (Bretherton et al. 2004) and instantaneous timescales (Peters and Neelin 2006) and explorations of this continue (e.g., Rushley et al. 2018; Wolding et al. 2020). For regions dominated by deep convection, this empirical relationship can be understood by computing the buoyancy of entraining plumes (Holloway and Neelin 2009; Schiro et al. 2016), which are consistent with observations provided the plume is allowed to entrain environmental air through a deep lower tropospheric layer.

The precipitation-moisture relationship shows dependence on column temperature (Neelin et al. 2009; Kuo et al. 2020), land surface (Ahmed and Schumacher 2017) and the land-sea interface (Bergemann and Jakob 2016). Figure 3a shows one way of quantifying this. Column water vapor (CWV) is used as a measure of moisture since satellite microwave retrievals are widely available over oceans (e.g., Hilburn and Wentz 2008). Temperature is measured by the column-integrated saturation value \hat{q}_{sat} from reanalysis (Kanamitsu et al. 2002) (other bulk measures of tropospheric temperature work similarly). For the range of temperatures relevant to the tropics, the dependence on moisture can be collapsed to a common form for all temperatures, when the water vapor is taken relative to a critical value w_c . This value characterizes the rapid increase of precipitation associated with the onset of convective conditional instability, with the difference $(CWV - w_c)$ acting like a crude measure of buoyancy, albeit with errors due to the presence of more detailed vertical structure than these bulk variables can capture. Percentiles of precipitation (from TRMM precipitation radar, coarse-grained to the CWV grid as in (Kuo et al. 2020) as a function of $(CWV - w_c)$ behave similarly for each temperature. The 50th percentile behaves similarly to the conditional average, exhibiting a rapid pickup above the critical value; higher percentiles have a corresponding rapid pickup in parallel with this.

Much of the moisture-temperature dependence is explainable if the moisture and temperature variations are

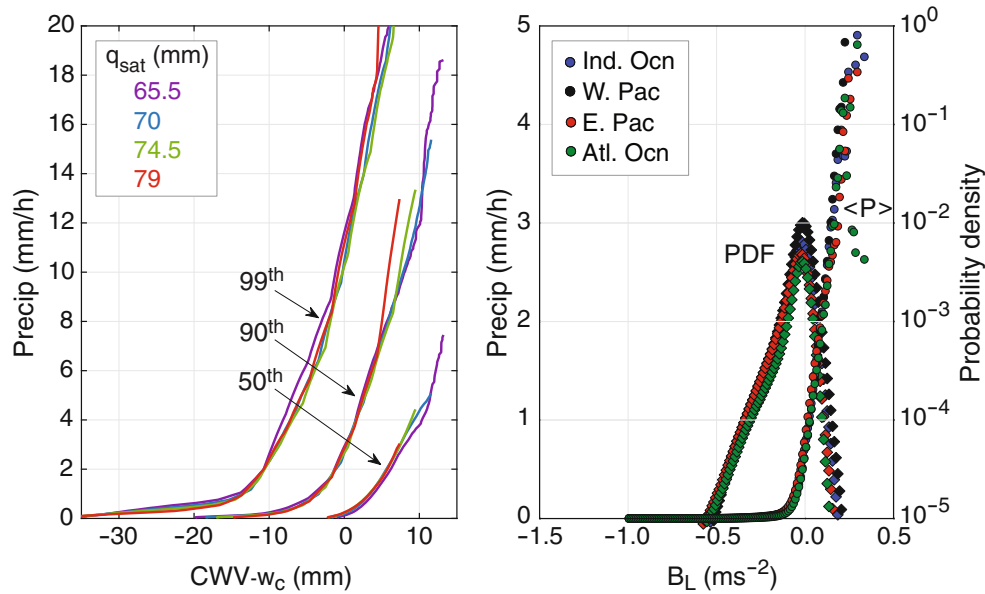


Fig. 3 Two ways of quantifying the relationship of precipitation to its moisture-temperature environment. **a** Precipitation percentiles as a function of column water vapor (CWV) relative to a critical value w_c that depends on temperature, here measured by the column-integrated saturation humidity \hat{q}_{sat} . $CWV-w_c(\hat{q}_{sat})$ acts as a rough proxy for buoyancy of convective plumes, yielding a

rapid pickup in precipitation percentiles or conditional average in the vicinity of the critical value that is similar for all temperatures (Kuo et al. 2018). **b** TRMM 3B42 precipitation conditionally averaged by an empirical estimator of plume buoyancy B_L for four different tropical ocean basins (left axis) and the pdfs of B_L (right axis)

mapped onto to a measure of cloud buoyancy (Ahmed and Neelin 2018; Schiro et al. 2018; Adames et al. 2021). The resulting precipitation-buoyancy relationship is valid across a wide range of environments, and is therefore a generalized version of the precipitation-moisture relationship—essentially acting like an empirical precipitation parameterization. Figure 3b depicts this buoyancy relationship, where tropical oceanic precipitation is conditionally averaged by a measure of lower tropospheric buoyancy (B_L). The probability density functions (pdfs) of B_L are sharply peaked near the value beyond which the conditional precipitation increases linearly.

Figure 3 suggests a simple empirical precipitation parameterization in which a threshold buoyancy value (B_c) separates the non-precipitating and precipitating regimes, and the linear precipitating regime is characterized by its slope, α :

$$P = \begin{cases} \alpha(B_L - B_c), & \text{if } B_L > B_c \\ 0, & \text{if } B_L \leq B_c. \end{cases} \quad (10)$$

The use of B_L provides a framework to understand the sensitivity of precipitation to changes in its thermodynamic environment. Following Ahmed et al. (2020), we can decompose B_L into two terms:

$$B_L = CAPE_L - SUBSAT_L. \quad (11)$$

In (11), $CAPE_L$ is akin to the commonly used convectively available potential energy (CAPE) and depends on the

difference between the boundary layer moist enthalpy and the free-tropospheric temperature, acting like a lower tropospheric static stability. The decreases in cloud buoyancy due to entrainment of dry air are captured by $SUBSAT_L$. The empirical buoyancy framework therefore quantifies the joint influence (Louf et al. 2019; Powell 2019; Tian and Kuang 2019) of moisture and CAPE on precipitation.

The buoyancy framework can be used to study precipitation distributions, provided one has knowledge of B_L evolution. The problem can be simplified by assuming that $CAPE_L$ remains fixed, so that B_L variations can be tracked purely by moisture variations. Under this assumption, the buoyancy threshold for precipitation, B_c , is transformed into a moisture threshold, q_c . This simple—but empirically rooted—precipitation parameterization can then be coupled to equally simple evolution equations for the environmental thermodynamics. Surprisingly, this has implications for probabilities of precipitation extremes, as outlined in the following section.

How Precipitation Distributions Arise: Variations Across a Moisture/Buoyancy Threshold

Denoting the size of a precipitation event as \mathcal{S} , measured in units of mm, a key quantity of interest is the pdf $p_s(\mathcal{S})$ of event sizes. The event size pdf can be measured from

observational data or climate model data (Peters et al. 2002; Neelin et al. 2008; Peters et al. 2010; Deluca and Corral 2014; Neelin et al. 2017; Martinez-Villalobos and Neelin 2018), and has been seen to take the form

$$p_s(\mathcal{S}) \propto \mathcal{S}^{-\tau} \exp[-\mathcal{S}/\mathcal{S}_L], \quad (12)$$

which includes a power law range due to $\mathcal{S}^{-\tau}$, and an exponential decay $\exp[-\mathcal{S}/\mathcal{S}_L]$ that becomes significant for the largest events beyond a large cutoff size \mathcal{S}_L (Stechmann and Neelin 2011, 2014; Neelin et al. 2017). See Fig. 4 for an illustration of the pdf from observational data.

Also shown in Fig. 4 is the pdf for a related quantity, the daily precipitation, i.e., the amount of precipitation P that falls in one day, whose pdf has a less-steep, approximately power law range. The power law range is slightly less steep in the midlatitude compared to the tropical case (in part due to 1-h vs 1-m data), but the pdf still shows essentially the same functional form. There is a long history of approximating rainfall distributions for daily average intensities (or similar averaging interval) as a gamma distribution

$$p_P(P) \propto P^{-\tau_P} \exp[-P/P_L], \quad \tau_P < 1 \quad (13)$$

(Barger and Thom 1949; Thom 1958; Groisman et al. 1999) including for projections of changes under warming (Wilby and Wigley 2002; Watterson and Dix 2003) (noting that some related distributions have also been used (Papalexiou and Koutsoyiannis 2013; O’Gorman 2014; Kirchmeier-Young et al. 2016; Moustakis et al. 2021)). We are now in a position to explain the physics behind this, beginning with an explanation of the event accumulation size distribution, which is simpler because it involves only the precipitating regime.

Why does the event size pdf take the form of (12)? A theory can be described using some of the intuition from previous sections (Stechmann and Neelin 2011, 2014; Hottovy and Stechmann 2015b, Neelin et al. 2017). Two important ingredients are (1) the threshold provided by the rapid onset in (10) and Fig. 3, and (2) variations across that threshold. To see this, consider the evolution equation for vertically integrated moisture from (1a), and write it in approximate form as

$$dq = -Pdt + \tilde{D}^{1/2}d\tilde{W}_t, \quad (14)$$

where the moisture convergence $\langle \nabla \cdot \mathbf{v}q \rangle$ and evaporation E have been approximated by white noise. The parameterization of P could be as in (10), which indicates the first important ingredient: a threshold in buoyancy and therefore in moisture. The second important ingredient is that the evolution in (14) governs the variations in both non-precipitating and precipitating regimes.

To arrive at the event size pdf in (12), consider the evolution of moisture, according to (14), at the start of a

precipitation event. Prior to the start of the event, $P = 0$ in (14). At the start of the event, P turns on, and one can replace time with a running accumulation $\tilde{\mathcal{S}}$, i.e., the amount of water rained out up to time t within an event:

$$\tilde{\mathcal{S}}(t) = \int_{t_0}^t P(t')dt', \quad \text{i.e.,} \quad d\tilde{\mathcal{S}} = Pdt. \quad (15)$$

The size \mathcal{S} of an event is simply the value of the running accumulation $\tilde{\mathcal{S}}$ when the event terminates. Since $d\tilde{\mathcal{S}} = Pdt$, one can rewrite (14) as

$$dq = -d\tilde{\mathcal{S}} + D^{1/2}dW_{\tilde{\mathcal{S}}}. \quad (16)$$

The event size \mathcal{S} can now be viewed as the “time” elapsed in waiting for moisture to decrease below a threshold value, similar to the threshold in (10), at which point the precipitation terminates. This is a first-passage-time problem for the stochastic differential equation in (16), and it can be solved analytically for the event size pdf $p_s(\mathcal{S})$, leading to the form shown in (12) (Gardiner 2009; Stechmann and Neelin 2014). Intuitively, the two parts of the pdf—the power law $\mathcal{S}^{-\tau}$ and the exponential decay $\exp[-\mathcal{S}/\mathcal{S}_L]$ —arise from the two parts of the stochastic evolution in (14). In particular, the stochastic variability from $\tilde{D}^{1/2}d\tilde{W}_t$ leads to the power law by the random crossing of a threshold, and after enough time has elapsed, the precipitation loss $-Pdt$ becomes more important and eventually cuts off the power law. These two processes are of equal importance at the cutoff scale, \mathcal{S}_L .

While physically accumulations (from event onset to termination) provide a more fundamental connection between the moisture budget and precipitation pdfs, in practice precipitation aggregated over fixed time intervals (e.g., daily precipitation) is the main object of the research community interest. An important distinction between event accumulation and daily precipitation is that the accumulation only depends on dynamics occurring while precipitating whereas daily precipitation mixes dynamics occurring at wet and dry times. This distinction has an important imprint in the resulting accumulation and daily precipitation pdfs. Figure 4 shows the typical shape of these pdfs for one location in the tropics (Fig. 4a) and one location in midlatitudes (Fig. 4b). In both cases pdfs display a power law range for low and moderate values and a cutoff scale where the probability drops much faster, in agreement with the stochastic prototype for accumulations. The main difference is the gentler power law exponent τ_P for daily precipitation ($\tau_P < \tau$), which can be explained using the stochastic prototype for accumulations as a starting point. Under suitable conditions for the length of accumulation events with respect to the averaging interval (e.g., 1 day for daily precipitation), daily precipitation is approximately the summation of individual accumulation events within a day. This reduces daily precipitation power law exponent

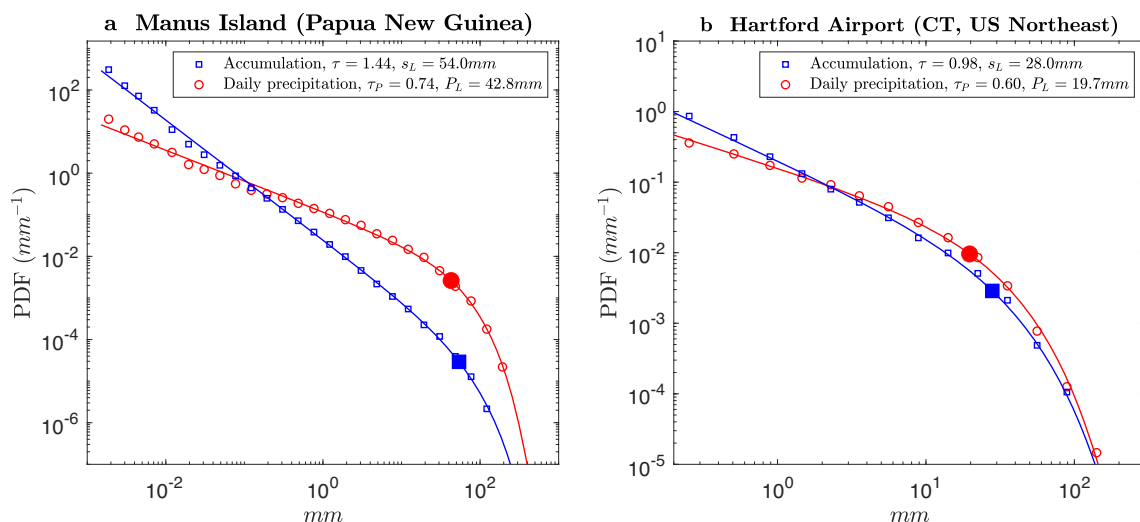


Fig. 4 Example of accumulation and daily precipitation pdfs in (a) a location in the tropics (Manus Island, 2° 3' S, 147° 25' E) and (b) mid-latitudes (Hartford Airport, CT, USA, 41° 56' N, 287° 19' E). Manus Island pdfs calculated from 1-min data quantized at 0.1 $\frac{mm}{min}$ intervals.

Hartford Airport pdfs calculated from 1-h data quantized at 0.254 $\frac{mm}{h}$ intervals. Blue and red circles denote the location of the accumulation cutoff S_L and daily precipitation cutoff P_L , respectively. Adapted from Martinez-Villalobos and Neelin (2019)

because days with multiple accumulation events contribute to a larger probability of higher daily precipitation amounts at the expense of low and moderate amounts, flattening the power law range (Martinez-Villalobos and Neelin 2019). The daily precipitation cutoff scale P_L is set by the underlying accumulation cutoff scale S_L (confirmed in observations over the USA, see Martinez-Villalobos and Neelin 2018), implying that daily precipitation extremes are approximately controlled by the same balances (fluctuations in moisture convergence vs moisture loss by precipitation) as accumulation extremes (Martinez-Villalobos and Neelin 2019).

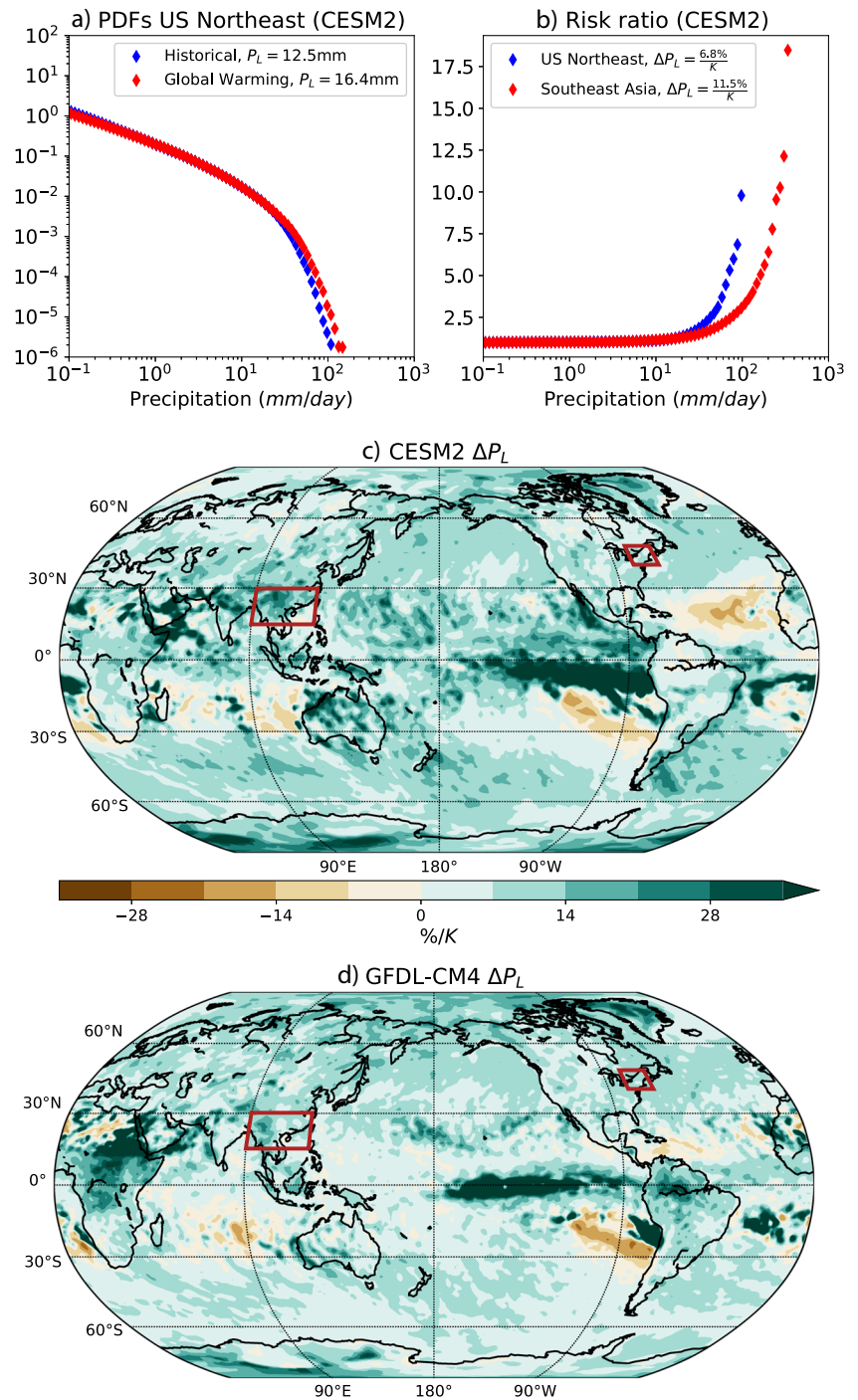
Climate models are known to exhibit errors in the current climate simulation of precipitation distributions, including too-frequent occurrences of low intensity rain (Hagos et al. 2021), and considerable differences at high percentiles (Pendergrass and Hartmann 2014; Goldenson et al. 2021; Norris et al. 2021; Fiedler et al. 2020). While marginal improvements are noted in Coupled Model Intercomparison Project Phase 6 (CMIP6) over earlier CMIP5 models in simulating precipitation extremes, inter-model spread and biases persist in the latest generation of models (Chen et al. 2020; Ha et al. 2020; Kim et al. 2020; Scoccimarro and Gualdi 2020; Wehner et al. 2020; Wehner 2020; Zhu et al. 2020; Chen et al. 2021; Li et al. 2021). How can the new connection of the precipitation intensity pdf to the thermodynamic environment inform this discussion? First, it suggests that the low-to-medium range intensity errors could be associated with a deficiency of variability, or an insufficiently sharp onset of precipitation as a function of moisture and temperature—both of which can occur in models. Second, it suggests that both of these factors affect

the physical precipitation scale P_L , governing the medium-to-high intensity range. This is consistent with the impact of resolution increases (Roberts et al. 2018; Wehner et al. 2014), increasing P_L while maintaining the shape of the medium-high intensity range, and of stochastic convective parameterization (Wang et al. 2021) which improves both ranges. In CMIP6 models (Martinez-Villalobos and Neelin 2021), the observed shape of the medium-high intensity range, and the spatial and seasonal changes in P_L are proportional to observed, yielding encouraging indications that fractional changes in the extreme events distribution may be reliable despite inter-model differences in the absolute value of this key parameter.

How Precipitation Distributions Change: Changes in Extremes

Physical insight from the stochastic prototype points to a single precipitation scale for accumulation (S_L) and daily precipitation (P_L) that encapsulate dynamical and thermodynamical effects for extremes. Because both thermodynamic and dynamic effects enter into the same cutoff scale (S_L , or P_L), this scale provides a useful test, in a single quantity, of both thermodynamic and dynamic effects. In comparison to the common use of percentiles, one advantage of using the cutoff scale P_L for extreme precipitation change assessment is that it is a more fundamental quantity, whose physics and connection to the moisture budget are relatively well understood, as outlined in the Section “How Precipitation Distributions Arise: Variations Across a Moisture/Buoyancy Threshold”.

Fig. 5 Examples of changes in key aspects of precipitation pdfs under warming. **a** US Northeast daily precipitation pdfs in CESM2 simulated for historical (blue; 1990–2014) and end-of-century (red; 2075–2099) SSP5-8.5 scenario radiative forcing. Note increases in the extreme tail under global warming associated with an increase in the precipitation scale P_L . **b** Daily precipitation risk ratios in two different regions (indicated by red boxes in **c**) for CESM2. Systematic increases for the largest events are controlled by ΔP_L versus P_L . **c** Percent change in P_L between 2075–2099 compared to 1990–2014 in CESM2. **d** Same as **a** but for GFDL-CM4. The $7\% \text{ K}^{-1}$ contour interval corresponds approximately to multiples of CC scaling



The scale P_L is also less affected than percentiles by the low-to-moderate range of the distribution for which models can exhibit substantial deficiencies (Pendergrass and Hartmann 2014; Hagos et al. 2021). We thus illustrate changes from example CMIP6 models in terms of this view of the distribution, and use it as a lens to review prior results.

For daily precipitation, Fig. 5a shows the pdf for an example region. Increases in P_L with warming tend to stretch the pdf: the medium-large intensity regime where

the pdf drops steeply in Fig. 5a shifts accordingly. This results in large increases in the probability of extremes, which is exacerbated with event rareness, as noted in various forms in multiple studies (e.g., Kunkel et al. 2013; Fischer and Knutti 2016; Pendergrass 2018; Myhre et al. 2019; Li et al. 2019; Kirchmeier-Young and Zhang 2020), including assessments based on CMIP6 models (Li et al. 2020; Akinsanola et al. 2020; Gupta et al. 2020; Ge et al. 2021; Dong et al. 2021). This is illustrated in Fig. 5b, which

shows the risk ratio (ratio between future and historical exceedances, conditioned on wet day occurrence) in two different regions in CESM2. In the US Northeast region (40°–48° N, 280°–293° E) the model shows a 10-fold increase in the probability of daily precipitation larger than about 100 mm (note logarithmic x -axis). A similar shape of the risk ratio occurs in the Southeast Asian region (15°–30° N, 90°–120° E) with increases in probability of almost 20 times for daily precipitation larger than 300 mm, consistent with the analysis in (Ge et al. 2021) over a similar region. Models' representation of this characteristic risk ratio shape is in agreement with theoretical findings (Martinez-Villalobos and Neelin 2019, Fig. 8), and mirror observed accumulation and daily precipitation risk ratios in the USA (Martinez-Villalobos and Neelin 2018) and China (Chang et al. 2020), as well as accumulation risk ratios in CESM1 (Neelin et al. 2017).

If the exponent of the approximately power law range does not change substantially, as illustrated in Fig. 5a, P_L governs a simple rescaling of the entire distribution. For event accumulations, this holds to high accuracy (Peters et al. 2010; Neelin et al. 2017) because this distribution involves only the precipitating regime. For daily average precipitation, this low-to-medium range tends to adjust slightly if the typical number of events per day changes, an effect governed by the dynamics of the non-precipitating intervals (Martinez-Villalobos and Neelin 2019). Even so, P_L governs the scaling of the large event range. Thus, maps of changes in daily precipitation cutoff scale P_L (Fig. 5c,d) for 2075–2099 under SSP5-8.5 (O'Neill et al. 2016) relative to historical conditions (1990–2014) summarize scaling as a function of region in two CMIP6 models (CESM2 and GFDL-CM4). Increases in P_L occur in most places with exception of some sub-tropical regions, as previously seen for high percentiles (Pall et al. 2007; Pfahl et al. 2017; Hoegh-Guldberg et al. 2018; Norris et al. 2019a). In midlatitudes, large areas tend to be roughly at CC scaling (alternating between slightly above and slightly below 7% K^{-1}), but ocean storm track regions tend to be consistently above CC. In sub-tropical dry regions there tend to be decreases or sub-CC scaling. However, in certain regions of the tropics, substantial areas of super-CC scaling by factors of 2 to exceeding 4 may be noted, although in the two examples shown, there is not good agreement on the specific spatial distribution of these. This summarizes, in a potentially more interpretable quantity, results seen in studies based on percentiles or other measures of extremes (Chen et al. 2021; Yin et al. 2021; Gupta et al. 2020).

Changes in organization of precipitation or in probability distributions that summarize aspects of convective organization have also been considered. One of the simplest behaviors is for area of clusters of contiguous precipitating points (Peters et al. 2009; Wood and Field 2011) or for

precipitation integrated over these clusters, termed cluster power. The probability distribution of tropical cluster power has a power law range followed by an approximately exponential cutoff in observations, which is reasonably simulated by climate models (Quinn and Neelin 2017a; 2017b). The cutoff scale increases in a warming climate, yielding probability increases for the largest clusters (Quinn and Neelin 2017b) analogous to those described for the distribution of precipitation accumulations or intensity. While quantitative changes vary among models, the tropical cutoff scale increase can be super-CC (Quinn and Neelin 2017a). Explanations for the distribution shape and for the physics of the cutoff scale are slightly more complex than for precipitation distribution discussed in the Section “[How Precipitation Distributions Arise: Variations Across a Moisture/Buoyancy Threshold](#)” due to the involvement of interactions between neighboring grid cells (Hottovy and Stechmann 2015a; Ahmed and Neelin 2019) but it appears to similarly be a physical scale governed by the moist physics of a climate model. Other results involving clusters can be more complex. In Chang et al. (2016), spatiotemporal clusters at midlatitudes over the USA exhibit partial compensation for increased intensity by reduced storm size.

Other effects not taken into account in the simple CC paradigm include the role of intermittency (Schleiss 2018; Visser et al. 2020) and the duration of precipitating events (Stechmann and Neelin 2014; Wasko et al. 2015; Norris et al. 2019b).

Discussion and Conclusions

There has been considerable progress in quantifying changes in precipitation distributions under warming as simulated in climate models. The default comparison has been to whether increases in high percentiles tend to scale proportional to expectations from Clausius-Clapeyron increases in moisture. There has been increasing recognition that departures from this scaling occur both in climate change simulations and within current observations. The sense that these must be associated with feedbacks from convective heating to the circulation is here summarized by showing that when the moisture and thermodynamic equations are considered together, such dynamical feedbacks should be expected unless specific conditions are met (Section “[“Thermodynamic” and Dynamical Contributions and Issues](#)”). In particular, for precipitation associated with convective conditions, which occur with large-scale moisture below saturation, such feedbacks are required by the combination of the moisture equation and thermodynamic equation. The common term “thermodynamic component” for changes associated with increased moisture alone can be severely misleading under these circumstances since

dynamical changes result from the need to satisfy thermodynamic balances.

In parallel with these developments, there has been progress in understanding the processes underlying precipitation probability distributions—including how they are shaped by their relationship to their thermodynamic environment in current climate. Dynamical insights from this can help clarify some of the factors at play in changes under global warming. In particular, these processes yield relatively simple basic postulates for the form of these changes.

As a pathway to further insight, it may be fruitful to bring together the various research threads described above. We have noted intriguing connections between the empirical exploration of super-CC scaling in the moisture-dependence of high percentiles and the onset of convection as a function of its thermodynamic environment, whether measured by water vapor and temperature, or by an empirical buoyancy variable (Section “[Precipitation Relationship to the Thermodynamic Environment](#)”). The role of the thermodynamic environment in dictating convective heating-convergence feedbacks through a gross moist stability may be valuable in understanding regions of super-CC scaling (the Sections “[Thermodynamic](#)” and [Dynamical Contributions and Issues](#)” and [Scaling Arguments](#)). Finally, the connection between key features of the precipitation probability distribution and fluctuations across the sharp onset threshold of precipitation given by the thermodynamic environment (the Section “[How Precipitation Distributions Arise: Variations Across a Moisture/Buoyancy Threshold](#)”) are only beginning to be exploited for the analysis of global climate models (the Section “[How Precipitation Distributions Change: Changes in Extremes](#)”). Quantities such as the precipitation scale—incorporating both dynamic and thermodynamic effects—that governs the medium-to-high intensity range for precipitation pdfs appear promising as tools for elucidating precipitation probability changes in global climate models.

Funding This work was supported in part by National Science Foundation grant AGS-1936810 and National Oceanic and Atmospheric Administration grant NA21OAR4310354 (JDN, FA, Y-HK, CM-V), by AGS-1742178 (GC), and by Proyecto Corfo Ingeniería 2030 código 14ENI2-26865 (CM-V).

Declarations

Conflict of Interest The authors declare that they have no conflict of interest.

Open Access This article is licensed under a Creative Commons Attribution 4.0 International License, which permits use, sharing, adaptation, distribution and reproduction in any medium or format, as long as you give appropriate credit to the original author(s) and the source, provide a link to the Creative Commons licence, and indicate if changes were made. The images or other third party material in this

article are included in the article’s Creative Commons licence, unless indicated otherwise in a credit line to the material. If material is not included in the article’s Creative Commons licence and your intended use is not permitted by statutory regulation or exceeds the permitted use, you will need to obtain permission directly from the copyright holder. To view a copy of this licence, visit <http://creativecommons.org/licenses/by/4.0/>.

References

- Abbott TH, Cronin TW, Beucler T. Convective dynamics and the response of precipitation extremes to warming in radiative-convective equilibrium. *J Atmos Sci.* 2020;77(5):1637–1660.
- Adames ÁF, Powell SW, Ahmed F, Mayta VC, Neelin JD. The evolution of tropical precipitation in an empirical buoyancy-based framework. *J Atmos Sci.* 2021;78:509–528. <https://doi.org/10.1175/JAS-D-20-0074.1>.
- Ahmed F, Adames AF, Neelin JD. Deep convective adjustment of temperature and moisture. *J Atmos Sci.* 2020;77:2163–2186. <https://doi.org/10.1175/JAS-D-19-0227.1>.
- Ahmed F, Neelin JD. Reverse engineering the tropical precipitation-buoyancy relationship. *J Atmos Sci.* 2018;75:1587–1608. <https://doi.org/10.1175/JAS-D-17-0333.1>.
- Ahmed F, Neelin JD. Explaining scales and statistics of tropical precipitation clusters with a stochastic model. *J Atmos Sci.* 2019;76:3063–3087. <https://doi.org/10.1175/JAS-D-18-0368.1>.
- Ahmed F, Schumacher C. Geographical differences in the tropical precipitation-moisture relationship and rain intensity onset. *Geophys Res Lett.* 2017;44(2):1114–1122.
- Akinsanola A, Kooperman G, Reed K, Pendergrass A, Hannah W. Projected changes in seasonal precipitation extremes over the United States in CMIP6 simulations. *Environ Res Lett.* 2020;15(10):104078.
- Allen MR, Ingram WJ. Constraints on future changes in climate and the hydrologic cycle. *Nature.* 2002;419(6903):224–232. <https://doi.org/10.1038/nature01092>.
- Attema JJ, Loriaux J, Lenderink G. Extreme precipitation response to climate perturbations in an atmospheric mesoscale model. *Environ Res Lett.* 2014;9(1):014003. <https://doi.org/10.1088/1748-9326/9/1/014003>.
- Back LE, Bretherton C. Geographic variability in the export of moist static energy and vertical motion profiles in the tropical pacific. *Geophys Res Lett.* 2006;33:L17810. <https://doi.org/10.1029/2006GL026672>.
- Barger GL, Thom HCS. Evaluation of drought hazard. *Agron J.* 1949;41(11):519. <https://doi.org/10.2134/agronj1949.00021962004100110004x>.
- Berg P, Moseley C, Haerter JO. Strong increase in convective precipitation in response to higher temperatures. *Nat Geosci.* 2013;6(3):181–185. <https://doi.org/10.1038/ngeo1731>.
- Bergemann M, Jakob C. How important is tropospheric humidity for coastal rainfall in the tropics? *Geophys Res Lett.* 2016;43(11):5860–5868.
- Bernstein DN, Neelin JD. Identifying sensitive ranges in global warming precipitation change dependence on convective parameters. *Geophys Res Lett.* 2016;43:5841–5850. <https://doi.org/10.1002/2016GL069022>.
- Biasutti M, Sobel AH, Kushnir Y. AGCM precipitation biases in the tropical Atlantic. *J Clim.* 2006;19:935–958.
- Biasutti M, Voigt A, Boos WR, Braconnot P, Hargreaves JC, Harrison SP, Kang SM, Mapes BE, Scheff J, Schumacher C, et al. Global energetics and local physics as drivers of past, present and future monsoons. *Nat Geosci.* 2018;11(6):392–400.

- Bony S, Dufresne JL, Treut HL, Morcrette JJ, Senior C. On dynamic and thermodynamic components of cloud changes. *Clim Dyn*. 2004;22:71–86. <https://doi.org/10.1007/s00382-003-0369-6>.
- Bretherton C, Peters ME, Back LE. Relationships between water vapor path and precipitation over the tropical oceans. *J Clim*. 2004;17:1517–1528.
- Chang M, Liu B, Martinez-Villalobos C, Ren G, Li S, Zhou T. Changes in extreme precipitation accumulations during the warm season over continental China. *J Clim*. 2020;33(24):10799–10811. <https://doi.org/10.1175/jcli-d-20-0616.1>.
- Chang W, Stein ML, Wang J, Kotamarthi VR, Moyer EJ. Changes in spatiotemporal precipitation patterns in changing climate conditions. *J Clim*. 2016;29(23):8355–8376.
- Chen CA, Hsu HH, Liang HC. Evaluation and comparison of CMIP6 and CMIP5 model performance in simulating the seasonal extreme precipitation in the Western North Pacific and East Asia. *Weather Clim Extremes*. 2021;31:100303.
- Chen G, Norris J, Neelin JD, Lu J, Leung LR, Sakaguchi K. Thermodynamic and dynamic mechanisms for hydrological cycle intensification over the full probability distribution of precipitation events. *J Atmos Sci*. 2019;76:497–516. <https://doi.org/10.1175/JAS-D-18-0067.1>.
- Chen H, Sun J, Lin W, Xu H. Comparison of CMIP6 and CMIP5 models in simulating climate extremes. *Sci Bulletin*. 2020;65(17):1415–1418.
- Chen Y, Li W, Jiang X, Zhai P, Luo Y. Detectable intensification of hourly and daily scale precipitation extremes across Eastern China. *J Clim*. 2021;34(3):1185–1201.
- Chou C, Chen CA, Tan PH, Chen KT. Mechanisms for global warming impacts on precipitation frequency and intensity. *J Clim*. 2012;25:3291–3306. <https://doi.org/10.1175/JCLI-D-11-00239.1>.
- Chou C, Neelin JD. Mechanisms of global warming impacts on regional tropical precipitation. *J Clim*. 2004;17:2688–2701.
- Covey C, Lucas D, Tannahill J, Garaizar X, Klein R. Efficient screening of climate model sensitivity to a large number of perturbed input parameters. *J Adv Model Earth Syst*. 2013;5:598–610. <https://doi.org/10.1002/jame.20040>.
- Deluca A, Corral A. Scale invariant events and dry spells for medium-resolution local rain data. *Nonlinear Process Geophys*. 2014;21:555–567. <https://doi.org/10.5194/npg-21-555-2014>.
- Donat MG, Sillmann J, Fischer EM. Changes in climate extremes in observations and climate model simulations. from the past to the future. In: *Climate extremes and their implications for impact and risk assessment*. Elsevier; 2020. p. 31–57.
- Dong S, Sun Y, Li C, Zhang X, Min SK, Kim YH. Attribution of extreme precipitation with updated observations and CMIP6 simulations. *J Clim*. 2021;34(3):871–881.
- Eden JM, Wolter K, Otto FE, Van Oldenborgh GJ. Multi-method attribution analysis of extreme precipitation in boulder, colorado. *Environ Res Lett*. 2016;11(12):124009.
- Emanuel K. Assessing the present and future probability of Hurricane Harvey's rainfall. *Proc Natl Acad Sci*. 2017;114(48):12681–12684.
- Emori S, Brown S. Dynamic and thermodynamic changes in mean and extreme precipitation under changed climate. *Geophys Res Lett*. 2005;32:L17706. <https://doi.org/10.1029/2005GL023272>.
- Fiedler S, Crueger T, D'Agostino R, Peters K, Becker T, Leutwyler D, Paccini L, Burdanowitz J, Buehler SA, Cortes AU, Dauhut T, Dommengot D, Fraedrich K, Jungandreas L, Maher N, Naumann AK, Rugenstein M, Sakradzija M, Schmidt H, Sielmann F, Stephan C, Timmreck C, Zhu X, Stevens B. Simulated tropical precipitation assessed across three major phases of the Coupled Model Intercomparison Project (CMIP). *Monthly Weather Rev*. 2020;148(9):3653–3680. <https://doi.org/10.1175/MWR-D-19-0404.1>.
- Fischer EM, Knutti R. Observed heavy precipitation increase confirms theory and early models. *Nat Clim Chang*. 2016;6(11):986–991. <https://doi.org/10.1038/nclimate3110>.
- Fowler HJ, Lenderink G, Prein AF, Westra S, Allan RP, Ban N, Barbero R, Berg P, Blenkinsop S, Do HX, Guerreiro S, Haerter JO, Kendon EJ, Lewis E, Schaer C, Sharma A, Villarini G, Wasko C, Zhang X. Anthropogenic intensification of short-duration rainfall extremes. *Nat Rev Earth Environ*. 2021;2(2):107–122. <https://doi.org/10.1038/s43017-020-00128-6>.
- Gardiner C. *Stochastic methods: a handbook for the natural and social sciences*, 4th ed. Berlin: Springer Series in Synergetics. Springer; 2009.
- Ge F, Zhu S, Luo H, Zhi X, Wang H. Future changes in precipitation extremes over Southeast Asia: insights from CMIP6 multi-model ensemble. *Environ Res Lett*. 2021;16(2):024013.
- Gimeno L, Nieto R, Vázquez M, Lavers D. Atmospheric rivers: a mini-review. *Front Earth Sci*. 2014;2:2.
- Goldenson N, Thackeray C, Hall A, Swain D, Berg N. Using large ensembles to identify regions of systematic biases in moderate to heavy daily precipitation. *Geophys Res Lett*. e2020GL092026. 2021.
- Groisman PY, Karl TR, Easterling DR, Knight RW, Jamason PF, Hennessy KJ, Suppiah R, Page CM, Wibig J, Fortuniak K, Razuvaev VN, Douglas A, Førland E, Zhai PM. Changes in the Probability of Heavy Precipitation: Important Indicators of Climatic Change. *Clim Chang*. 1999;42(1):243–283. <https://doi.org/10.1023/A:1005432803188>.
- Gupta V, Singh V, Jain MK. Assessment of precipitation extremes in India during the 21st century under SSP1-1.9 mitigation scenarios of CMIP6 GCMs. *J Hydrol*. 2020;590:125422.
- Ha KJ, Moon S, Timmermann A, Kim D. Future changes of summer monsoon characteristics and evaporative demand over Asia in CMIP6 simulations. *Geophys Res Lett*. 2020;47(8):e2020GL087492.
- Haerter JO, Berg P. Unexpected rise in extreme precipitation caused by a shift in rain type?. *Nat Geosci*. 2009;2(6):372–373. <https://doi.org/10.1038/ngeo523>.
- Haerter JO, Schlemmer L. Intensified cold pool dynamics under stronger surface heating. *Geophys Res Lett*. 2018;45(12):6299–6310. <https://doi.org/10.1029/2017GL076874>.
- Hagos SM, Leung LR, Garuba OA, Demott C, Harrop B, Lu J, Ahn MS. The relationship between precipitation and precipitable water in CMIP6 simulations and implications for tropical climatology and change. *J Clim*. 2021;34(5):1587–1600.
- Haustein K, Otto F, Uhe P, Schaller N, Allen M, Hermanson L, Christidis N, McLean P, Cullen H. Real-time extreme weather event attribution with forecast seasonal SSTs. *Environ Res Lett*. 2016;11(6):064006.
- Held IM, Soden BJ. Robust responses of the hydrological cycle to global warming. *J Clim*. 2006;19:5686–5699.
- Hilburn KA, Wentz FJ. Intercalibrated passive microwave rain products from the Unified Microwave Ocean Retrieval Algorithm (UMORA). *J Appl Meteor*. 2008;25:778–794.
- Hoegh-Guldberg O, Jacob D, Taylor M, Bindi M, Brown S, Camilloni I, Diedhiou A, Djalante R, Ebi K, Engelbrecht F, et al. Impacts of 1.5° C global warming on natural and human systems. In: *Global warming of 1.5°C: an IPCC special report*. IPCC secretariat; 2018. p. 175–311.
- Holloway CE, Neelin JD. Moisture vertical structure, column water vapor, and tropical deep convection. *J Atmos Sci*. 2009;66:1665–1683.
- Holloway CE, Neelin JD. Temporal relations of column water vapor and tropical precipitation. *J Atmos Sci*. 2010;67:1091–1105. <https://doi.org/10.1175/2009JAS3284.1>.

- Hottovy S, Stechmann S. A spatiotemporal stochastic model for tropical precipitation and water vapor dynamics. *J Atmos Sci*. 2015;72(12):4721–4738. <https://doi.org/10.1175/JAS-D-15-0119.1>.
- Hottovy S, Stechmann S. Threshold models for rainfall and convection: Deterministic versus stochastic triggers. *SIAM J Appl Math*. 2015;75:861–884. <https://doi.org/10.1137/140980788>.
- Inoue K, Back LE. Gross moist stability assessment during TOGA COARE: Various interpretations of gross moist stability. *J Atmos Sci*. 2015;72(11):4148–4166.
- Inoue K, Back LE. Gross moist stability analysis: Assessment of satellite-based products in the GMS plane. *J Atmos Sci*. 2017;74(6):1819–1837.
- Kanamitsu M, Ebisuzaki W, Woollen J, Yang SK, Hnilo J, Fiorino M, Potter G. NCEP–DOE AMIP-II reanalysis (R-2). *Bull Am Meteorol Soc*. 2002;83(11):1631–1644.
- Kim YH, Min SK, Zhang X, Sillmann J, Sandstad M. Evaluation of the CMIP6 multi-model ensemble for climate extreme indices. *Weather Clim Extremes*. 2020;29:100269.
- Kirchmeier-Young MC, Lorenz DJ, Vimont DJ. Extreme event verification for probabilistic downscaling. *J Appl Meteorol Climatol*. 2016;55(11):2411–2430. <https://doi.org/10.1175/JAMC-D-16-0043.1>.
- Kirchmeier-Young MC, Zhang X. Human influence has intensified extreme precipitation in North America. *Proc Natl Acad Sci*. 2020;117(24):13308–13313. <https://doi.org/10.1073/pnas.1921628117>.
- Knight CG, Knight SHE, Massey N, Aina T, Christensen C, Frame DJ, Kettleborough JA, Martin A, Pascoe S, Sanderson B, Stainforth DA, Allen MR. Association of parameter, software, and hardware variation with large-scale behavior across 57,000 climate models. *Proc Nat Acad Sci*. 2007;104:12259–12264. <https://doi.org/10.1175/JCLI3430.1>.
- Kunkel K, Karl TR, Brooks H, Kossin J, Lawrimore JH, Arndt D, Bosart L, Changnon D, Cutter SL, Doesken N, Emanuel K, Groisman PY, Katz RW, Knutson T, O'Brien J, Paciorek C, Peterson TC, Redmond K, Robinson D, Trapp J, Vose R, Weaver S, Wehner M, Wolter K, Wuebbles D. Monitoring and understanding trends in extreme storms: State of knowledge. *Bull Am Meteorol Soc*. 2013;94(4):499–514. <https://doi.org/10.1175/BAMS-D-11-00262.1>.
- Kuo YH, Neelin JD, Booth JF, Chen CC, Chen WT, Gettelman A, Jiang X, Maloney E, Mechoso CR, Ming Y, Schiro K, Seman CJ, Wu CM, Zhao M. Convective transition statistics over tropical oceans for climate model diagnostics: GCM evaluation. *J Atmos Sci*. 2020;77:379–403. <https://doi.org/10.1175/JAS-D-19-0132.1>.
- Kuo YH, Neelin JD, Schiro K. Convective transition statistics over tropical oceans for climate model diagnostics: Observational baseline. *J Atmos Sci*. 2018;75:1553–1570. <https://doi.org/10.1175/JAS-D-17-0287.1>.
- Lenderink G, Attema J. A simple scaling approach to produce climate scenarios of local precipitation extremes for the Netherlands. *Environ Res Lett*. 2015;10(8):085001.
- Lenderink G, Barbero R, Loriaux J, Fowler H. Super-Clausius–Clapeyron scaling of extreme hourly convective precipitation and its relation to large-scale atmospheric conditions. *J Clim*. 2017;30(15):6037–6052.
- Lenderink G, Barbero R, Westra S, Fowler HJ. Reply to comments on “Temperature-extreme precipitation scaling: a two-way causality?”. *Int J Climatol*. 2018;38:8–10. <https://doi.org/10.1002/joc.5799>.
- Lenderink G, Belušić D, Fowler HJ, Kjellström E, Lind P, van Meijgaard E, van Ulft B, de Vries H. Systematic increases in the thermodynamic response of hourly precipitation extremes in an idealized warming experiment with a convection-permitting climate model. *Environ Res Lett*. 2019;14(7):074012.
- Lenderink G, Van Meijgaard E. Increase in hourly precipitation extremes beyond expectations from temperature changes. *Nat Geosci*. 2008;1(8):511–514. <https://doi.org/10.1038/ngeo262>.
- Lenderink G, de Vries H, Fowler HJ, Barbero R, van Ulft B, van Meijgaard E. Scaling and responses of extreme hourly precipitation in three climate experiments with a convection-permitting model. *Philos Trans R Soc Math Phys Eng Sci*. 2021;379(2195):20190544. <https://doi.org/10.1098/rsta.2019.0544>.
- Li C, Zwiers F, Zhang X, Chen G, Lu J, Li G, Norris J, Tan Y, Sun Y, Liu M. Larger increases in more extreme local precipitation events as climate warms. *Geophys Res Lett*. 2019.
- Li C, Zwiers F, Zhang X, Li G, Sun Y, Wehner M. Changes in annual extremes of daily temperature and precipitation in CMIP6 models. *J Clim*. 1–61. 2020.
- Li Y, Yan D, Peng H, Xiao S. Evaluation of precipitation in CMIP6 over the Yangtze River basin. *Atmos Res*. 2021;253:105406.
- Li Z, O’Gorman P. Response of vertical velocities in extratropical precipitation extremes to climate change. *J Clim*. 2020;33(16):7125–7139.
- Lintner BR, Adams DK, Schiro K, Stansfield AM, da Rocha A, Neelin JD. Relationships among climatological vertical moisture structure, column water vapor, and precipitation over the central Amazon in observations and CMIP5 models. *Geophys Res Lett*. 2017;44:1981–1989. <https://doi.org/10.1002/2016GL071923>.
- Lochbihler K, Lenderink G, Siebesma AP. The spatial extent of rainfall events and its relation to precipitation scaling. *Geophys Res Lett*. 2017;44(16):8629–8636. <https://doi.org/10.1002/2017GL074857>.
- Lochbihler K, Lenderink G, Siebesma AP. Response of extreme precipitating cell structures to atmospheric warming. *J Geophys Res Atmospher*:2018JD029954. <https://doi.org/10.1029/2018JD029954>. 2019.
- Lochbihler K, Lenderink G, Siebesma AP. Cold Pool Dynamics Shape the Response of Extreme Rainfall Events to Climate Change. *J Adv Model Earth Syst*. 2021;13(2):1–16. <https://doi.org/10.1029/2020MS002306>.
- Loriaux JM, Lenderink G, De Roode SR, Siebesma AP. Understanding convective extreme precipitation scaling using observations and an entraining plume model. *J Atmospher Sci*. 2013;70(11):3641–3655.
- Louf V, Jakob C, Protat A, Bergemann M, Narsey S. The relationship of cloud number and size with their large-scale environment in deep tropical convection. *Geophys Res Lett*. 2019;46(15):9203–9212.
- Ma W, Norris J, Chen G. Projected changes to extreme precipitation along North American West Coast from the CESM large ensemble. *Geophys Res Lett*. 2019.
- Martinez-Villalobos C, Neelin JD. Shifts in precipitation accumulation distributions during the warm season over the United States. *Geophys Res Lett*. 2018;45:8586–8595. <https://doi.org/10.1029/2018GL078465>.
- Martinez-Villalobos C, Neelin JD. Why do precipitation intensities tend to follow gamma distributions. *J Atmos Sci*. 2019;76:3611–3631. <https://doi.org/10.1175/JAS-D-18-0343.1>.
- Martinez-Villalobos C, Neelin JD. Global climate models capture key features of extreme precipitation probabilities across regions. *Environ Res Lett*. 2021;16:024017. <https://doi.org/10.1088/1748-9326/abd351>.
- Meehl G, Collins WD, Boville BA, Kiehl JT, Wigley TML, Arblaster J. Response of the NCAR climate system model to increased CO₂ and the role of physical processes. *J Clim*. 2000;13:1879–1898.

- Meinshausen M, Smith SJ, Calvin K, Daniel JS, Kainuma MLT, Lamarque J, Matsumoto K, Montzka SA, Raper S, Riahi K, Thomson A, Velders GJM, van Vuuren DPP. The RCP greenhouse gas concentrations and their extensions from 1765 to 2300. *Clim Chang*. 2011;109:213–241. <https://doi.org/10.1007/s10584-011-0156-z>.
- Min SK, Zhang X, Zwiers F, Hegerl GC. Human contribution to more intense precipitation extremes. *Nature*. 2011;470:378–381.
- Moustakis Y, Papalexioiu SM, Onof CJ, Paschalis A. Seasonality, intensity, and duration of rainfall extremes change in a warmer climate. *Earth's Fut*:9(3). 2021.
- Muller C, O’Gorman P. An energetic perspective on the regional response of precipitation to climate change. *Nat Clim Chang*. 2011;1(5):266–271.
- Muller CJ, O’Gorman P, Back LE. Intensification of precipitation extremes with warming in a cloud-resolving model. *J Clim*. 2011;24(11):2784–2800.
- Muller CJ, Takayabu Y. Response of precipitation extremes to warming: what have we learned from theory and idealized cloud-resolving simulations, and what remains to be learned? *Environ Res Lett*. 2020.
- Myhre G, Alterskjær K, Stjern CW, Hodnebrog Ø, Marelle L, Samset BH, Sillmann J, Schaller N, Fischer E, Schulz M, et al. Frequency of extreme precipitation increases extensively with event rareness under global warming. *Sci Rep*. 2019;9(1):1–10.
- Neelin JD. The Global Circulation of the Atmosphere, chap. Moist dynamics of tropical convection zones in monsoons, teleconnections and global warming. Princeton: Princeton University Press; 2007, pp. 267–301.
- Neelin JD, Held IM. Modelling, tropical convergence based on the moist static energy budget. *Mon Wea Rev*. 1987;115:3–12.
- Neelin JD, Peters O, Hales K. The transition to strong convection. *J Atmos Sci*. 2009;66:2367–2384.
- Neelin JD, Peters O, Lin JWB, Hales K, Holloway CE. Rethinking convective quasi-equilibrium: observational constraints for stochastic convective schemes in climate models. *Phil Trans R Soc A*. 2008;366:2581–2604.
- Neelin JD, Sahany S, Stechmann S, Bernstein DN. Global warming precipitation accumulation increases above the current-climate cutoff scale. *Proc Nat Acad Sci*. 2017;114:1258–1263. <https://doi.org/10.1073/pnas.1615333114>.
- Neelin JD, Zeng N. A quasi-equilibrium tropical circulation model—formulation. *J Atmos Sci*. 2000;57:1741–1766.
- Nie J, Dai P, Sobel AH. Dry and moist dynamics shape regional patterns of extreme precipitation sensitivity. *Proc Ntl Acad Sci*. 2020;117(16):8757–8763.
- Nie J, Sobel AH, Shaevitz DA, Wang S. Dynamic amplification of extreme precipitation sensitivity. *Proc Ntl Acad Sci*. 2018;115(38):9467–9472.
- Noda A, Tokioka T. The effect of doubling the CO₂ concentration on convective and non-convective precipitation in a general circulation model coupled with a simple mixed layer ocean model. *J Meteorol Soc Jpn Ser II*. 1989;67(6):1057–1069.
- Norris J, Chen G, Neelin JD. Thermodynamic versus dynamic controls on extreme precipitation in a warming climate from the Community Earth System Model Large Ensemble. *J Clim*. 2019;32:1025–1045. <https://doi.org/10.1175/JCLI-D-18-0302.1>.
- Norris JM, Chen G, Neelin JD. Changes in frequency of large precipitation accumulations over land in a warming climate from the CESM large ensemble: the roles of moisture, circulation and duration. *J Clim*. 2019;32:5397–5416. <https://doi.org/10.1175/JCLI-D-18-0600.1>.
- Norris JM, Hall A, Neelin JD, Thackeray CW, Chen D. Evaluation of the tail of the probability distribution of daily and sub-daily precipitation in CMIP6 models. *J Clim* p. in press. <https://doi.org/10.1175/JCLI-D-20-0182.1>. 2021.
- O’Gorman P. Sensitivity of tropical precipitation extremes to climate change. *Nat Geosci*. 2012;5:697–700. <https://doi.org/10.1038/ngeo1568>.
- O’Gorman P. Contrasting responses of mean and extreme snowfall to climate change. *Nature*. 2014;512(7515):416–418. <https://doi.org/10.1038/nature13625>.
- O’Gorman P. Precipitation extremes under climate change. *Curr Clim Chang Rep*. 2015;1(2):49–59. <https://doi.org/10.1007/s40641-015-0009-3>.
- O’Gorman P, Schneider T. The physical basis for increases in precipitation extremes in simulations of 21st-century climate change. *Proc Ntl Acad Sci*. 2009;106(35):14773–14777. <https://doi.org/10.1073/pnas.0907610106>.
- van Oldenborgh GJ, van der Wiel K, Sebastian A, Singh R, Arrighi J, Otto F, Haustein K, Li S, Vecchi G, Cullen H. Attribution of extreme rainfall from Hurricane Harvey, August 2017. *Environ Res Lett*. 2017;12(12):124009. <https://doi.org/10.1088/1748-9326/aa9ef2>.
- Oueslati B, Yiou P, Jézéquel A. Revisiting the dynamic and thermodynamic processes driving the record-breaking january 2014 precipitation in the southern UK. *Sci Rep*. 2019;9(1):1–7.
- O’Gorman P, Li Z, Boos W, Yuval J. Response of extreme precipitation to uniform surface warming in quasi-global aquaplanet simulations at high resolution. *Philos Trans R Soc A*. 2021;379(2195):20190543.
- O’Gorman P, Schneider T. Scaling of precipitation extremes over a wide range of climates simulated with an idealized GCM. *J Clim*. 2009;22(21):5676–5685.
- O’Neill B, Tebaldi C, Van Vuuren D, Eyring V, Friedlingstein P, Hurtt G, Knutti R, Kriegler E, Lamarque J, Lowe J, et al. The Scenario Model Intercomparison Project (scenarioMIP) for CMIP6. *Geosci Model Dev*. 2016;9:3461–3482.
- Pall P, Allen MR, Stone DA. Testing the Clausius-Clapeyron constraint on changes in extreme precipitation under CO₂ warming. *Clim Dyn*. 2007;28:351–363. <https://doi.org/10.1007/s00382-006-0180-2>.
- Pall P, Patricola CM, Wehner M, Stone DA, Paciorek C, Collins WD. Diagnosing conditional anthropogenic contributions to heavy colorado rainfall in september 2013. *Weather Clim Extremes*. 2017;17:1–6.
- Papalexioiu SM, Koutsoyiannis D. Battle of extreme value distributions: A global survey on extreme daily rainfall. *Water Resour Res*. 2013;49(1):187–201. <https://doi.org/10.1029/2012WR012557>.
- Papalexioiu SM, Montanari A. Global and regional increase of precipitation extremes under global warming. *Water Resour Res*. 2019;55(6):4901–4914.
- Payne AE, Demory ME, Leung LR, Ramos AM, Shields CA, Rutz J, Siler N, Villarini G, Hall A, Ralph FM. Responses and impacts of atmospheric rivers to climate change. *Nat Revi Earth Environ*. 2020;1(3):143–157.
- Pendergrass A, Coleman D, Deser C, Lehner F, Rosenbloom N, Simpson I. Nonlinear response of extreme precipitation to warming in CESM1. *Geophys Res Lett*. 2019;46(17-18):10551–10560.
- Pendergrass AG. What precipitation is extreme?. *Science*. 2018;360(6393):1072–1073. <https://doi.org/10.1126/science.aat1871>.
- Pendergrass AG, Gerber EP. The rain is askew: Two idealized models relating vertical velocity and precipitation distributions in a warming world. *J Clim*. 2016;29(18):6445–6462. <https://doi.org/10.1175/JCLI-D-16-0097.1>.
- Pendergrass AG, Hartmann DL. Two modes of change of the distribution of rain. *J Clim*. 2014;27(22):8357–8371. <https://doi.org/10.1175/JCLI-D-14-00182.1>.
- Peters O, Deluca A, Corral A, Neelin JD, Holloway CE. Universality of rain event size distributions. *J Stat Mech*:P11030. <https://doi.org/10.1088/1742-5468/2010/11/P11030>. 2010.

- Peters O, Hertlein C, Christensen K. A complexity view of rainfall. *Phys Rev Lett*. 2002;88(1):018701. <https://doi.org/10.1103/PhysRevLett.88.018701>.
- Peters O, Neelin JD. Critical phenomena in atmospheric precipitation. *Nat Phys*. 2006;2:393–396. <https://doi.org/10.1038/nphys314>.
- Peters O, Neelin JD, Nesbitt SW. Mesoscale convective systems and critical clusters. *J Atmos Sci*. 2009;66:2913–2924. <https://doi.org/10.1175/2008JAS2761.1>.
- Pfahl S, O’Gorman P, Fischer EM. Understanding the regional pattern of projected future changes in extreme precipitation. *Nat Clim Chang*. 2017;7:423–427.
- Powell SW. Observing possible thermodynamic controls on tropical marine rainfall in moist environments. *J Atmos Sci*. 2019;76(12):3737–3751.
- Prein AF, Liu C, Ikeda K, Trier SB, Rasmussen RM, Holland GJ, Clark MP. Increased rainfall volume from future convective storms in the US. *Nat Clim Chang*. 2017;7(12):880–884. <https://doi.org/10.1038/s41558-017-0007-7>.
- Prein AF, Rasmussen RM, Ikeda K, Liu C, Clark MP, Holland GJ. The future intensification of hourly precipitation extremes. *Nat Clim Chang*. 2017;7(1):48–52. <https://doi.org/10.1038/nclim.ate3168>.
- Qian Y, Wan H, Yang B, Golaz JC, Harrop B, Hou Z, Larson VE, Leung LR, Lin G, Lin W, et al. Parametric sensitivity and uncertainty quantification in the version 1 of e3SM atmosphere model based on short perturbed parameter ensemble simulations. *J Geophys Res Atmospher*. 2018;123(23):13–046.
- Qian Y, Yan H, Hou Z, Johannesson G, Klein S, Lucas D, Neale R, Rasch P, Swiler L, Tannahill J, et al. Parametric sensitivity analysis of precipitation at global and local scales in the community atmosphere model CAM5. *J Adv Model Earth Syst*. 2015;7(2):382–411.
- Quinn KM, Neelin JD. Distributions of tropical precipitation cluster power and their changes under global warming. Part I: Observational baseline and comparison to a high-resolution atmospheric model. *J Clim*. 2017;30:8033–8044. <https://doi.org/10.1175/JCLI-D-16-0683.1>.
- Quinn KM, Neelin JD. Distributions of tropical precipitation cluster power and their changes under global warming. Part II: Long-term time-dependence in Coupled Model Intercomparison Project Phase 5 models. *J Clim*. 2017;30:8045–8059. <https://doi.org/10.1175/JCLI-D-16-0701.1>.
- Ralph FM, Dettinger M, Lavers D, Gorodetskaya IV, Martin A, Viale M, White AB, Oakley N, Rutz J, Spackman JR, et al. Atmospheric rivers emerge as a global science and applications focus. *Bull Am Meteorol Soc*. 2017;98(9):1969–1973.
- Raymond DJ, Sessions SL, Fuchs Ž. A theory for the spinup of tropical depressions. *Q J R Meteorol Soc*. 2007;133(628):1743–1754.
- Raymond DJ, Sessions SL, Sobel AH, Fuchs Ž. The mechanics of gross moist stability. *J Adv Model Earth Syst*:1(3). 2009.
- Risser MD, Wehner M. Attributable human-induced changes in the likelihood and magnitude of the observed extreme precipitation during Hurricane Harvey. *Geophys Res Lett*. 2017;44(24):12–457.
- Roberts M, Vidale P, Senior C, Hewitt H, Bates C, Berthou S, Chang P, Christensen H, Danilov S, Demory ME, et al. The benefits of global high resolution for climate simulation: process understanding and the enabling of stakeholder decisions at the regional scale. *Bull Am Meteorol Soc*. 2018;99(11):2341–2359.
- Rushley S, Kim D, Bretherton C, Ahn MS. Reexamining the nonlinear moisture-precipitation relationship over the tropical oceans. *Geophys Res Lett*. 2018;45(2):1133–1140.
- Sahany S, Neelin JD, Hales K, Neale RB. Deep convective transition characteristics in the Community Climate System Model and changes under global warming. *J Clim*. 2014;27:9214–9232. <https://doi.org/10.1175/JCLI-D-13-00747.1>.
- Sanderson BM. A multimodel study of parametric uncertainty in predictions of climate response to rising greenhouse gas concentrations. *J Clim*. 2011;24:1362–1377.
- Schiro K, Neelin JD, Adams DK, Lintner BR. Deep convection and column water vapor over tropical land vs. tropical ocean: A comparison between the Amazon and the Tropical Western Pacific. *J Atmos Sci*. 2016;73:4043–4063. <https://doi.org/10.1175/JAS-D-16-0119.1>.
- Schiro K, Ahmed F, Giangrande SE, Neelin JD. GoAmazon2014/5 campaign points to deep-inflow approach to deep convection across scales. *Proc Ntl Acad Sci*. 2018;115:201719842. <https://doi.org/10.1073/pnas.1719842115>.
- Schleiss M. How intermittency affects the rate at which rainfall extremes respond to changes in temperature. *Earth Syst Dyn*. 2018;9(3):955–968. <https://doi.org/10.5194/esd-9-955-2018>.
- Schneider T, O’Gorman P, Levine XJ. Water vapor and the dynamics of climate changes. *Rev Geophys*. 2010;48(3):RG3001. <https://doi.org/10.1029/2009RG000302>.
- Soccimarro E, Gualdi S. Heavy daily precipitation events in the CMIP6 worst-case scenario: Projected twenty-first-century changes. *J Clim*. 2020;33(17):7631–7642.
- Seager R, Neelin JD, Simpson IH, Henderson IN, Shaw T, Kushnir Y, Ting M. Dynamical and thermodynamical causes of large-scale changes in the hydrological cycle over North America, in response to global warming. *J Clim*. 2014;27:7921–7948. <https://doi.org/10.1175/JCLI-D-14-00153.1>.
- Sillmann J, Kharin VV, Zwiers F, Zhang X, Bronaughy D. Climate extremes indices in the CMIP5 multimodel ensemble: Part 2. Future climate projections. *J Geophys Res Atmos*. 2013;118:2473–2493. <https://doi.org/10.1002/jgrd.50188>.
- Singleton A, Toumi R. Super-Clausius-Clapeyron scaling of rainfall in a model squall line. *Q J R Meteorol Soc*. 2013;139(671):334–339. <https://doi.org/10.1002/qj.1919>.
- Stechmann S, Neelin JD. A stochastic model for the transition to strong convection. *J Atmos Sci*. 2011;68:2955–2970.
- Stechmann S, Neelin JD. First-passage-time prototypes for precipitation statistics. *J Atmos Sci*. 2014;71:3269–3291. <https://doi.org/10.1175/JAS-D-13-0268.1>.
- Sugiyama M, Shioyama H, Emori S. Precipitation extreme changes exceeding moisture content increases in MIROC and IPCC climate models. *PNAS*. 2010;107:571–575. <https://doi.org/10.1073/pnas.0903186107>.
- Tabari H. Climate change impact on flood and extreme precipitation increases with water availability. *Sci Rep*. 2020;10(1):1–10.
- Tandon NF, Zhang X, Sobel AH. Understanding the dynamics of future changes in extreme precipitation intensity. *Geophys Res Lett*. 2018;45:2870–2878.
- Tebaldi C, Hayhoe K, Arblaster J, Meehl G. Going to extremes. An intercomparison of model-simulated historical and future changes in extreme events. *Clim Chang*. 2006;79:185–211. <https://doi.org/10.1007/s10584-006-9051-4>.
- Thom HCS. A note on the Gamma distribution. *Monthly Weather Rev*. 1958;86(4):117–122. [https://doi.org/10.1175/1520-0493\(1958\)06<0117:ANOTGD>2.0.CO;2](https://doi.org/10.1175/1520-0493(1958)06<0117:ANOTGD>2.0.CO;2).
- Tian Y, Kuang Z. Why does deep convection have different sensitivities to temperature perturbations in the lower versus upper troposphere? *J Atmos Sci*. 2019;76(1):27–41.
- Tomassini L. The interaction between moist convection and the atmospheric circulation in the tropics. *Bull Am Meteorol Soc*. 2020;101(8):E1378–E1396.
- Trenberth KE. Changes in precipitation with climate change. *Clim Res*. 2011;47:123–138.

- Trenberth KE, Dai A, Rasmussen RM, Parsons DB. The changing character of precipitation. *Bull Amer Meteor Soc.* 2003;84:1205–1217.
- Valenzuela RA, Garreaud RD. Extreme daily rainfall in central-southern Chile and its relationship with low-level horizontal water vapor fluxes. *J Hydrometeorol.* 2019;20(9):1829–1850. <https://doi.org/10.1175/JHM-D-19-0036.1>.
- Visser JB, Wasko C, Sharma A, Nathan R. Resolving inconsistencies in extreme precipitation-temperature sensitivities. *Geophys Res Lett.* 2020;47(18):e2020GL089723. <https://doi.org/10.1029/2020GL089723>.
- Waliser D, Guan B. Extreme winds and precipitation during landfall of atmospheric rivers. *Nat Geosci.* 2017;10(3):179–183.
- Wang SS, Zhao L, Yoon JH, Klotzbach P, Gillies RR. Quantitative attribution of climate effects on Hurricane Harvey's extreme rainfall in Texas. *Environ Res Lett.* 2018;13(5):054014.
- Wang Y, Zhang GJ, Xie S, Lin W, Craig GC, Tang Q, Ma HY. Effects of coupling a stochastic convective parameterization with the Zhang–McFarlane scheme on precipitation simulation in the DOE e3SMv1.0 atmosphere model. *Geosci Model Dev.* 2021;14(3):1575–1593.
- Wasko C, Sharma A. Quantile regression for investigating scaling of extreme precipitation with temperature. *Water Resour Res.* 2014;50(4):3608–3614.
- Wasko C, Sharma A. Steeper temporal distribution of rain intensity at higher temperatures within Australian storms. *Nat Geosci.* 2015;8(7):527–529.
- Wasko C, Sharma A, Johnson F. Does storm duration modulate the extreme precipitation-temperature scaling relationship?. *Geophys Res Lett.* 2015;42(20):8783–8790. <https://doi.org/10.1002/2015GL066274>.
- Watterson IG, Dix MR. Simulated changes due to global warming in daily precipitation means and extremes and their interpretation using the gamma distribution. *J Geophys Res Atmospher.* 2003;108(D13):4379. <https://doi.org/10.1029/2002JD002928>.
- Wehner M, Gleckler P, Lee J. Characterization of long period return values of extreme daily temperature and precipitation in the CMIP6 models: Part 1, model evaluation. *Weather Clim Extremes.* 2020;30:100283.
- Wehner M. Characterization of long period return values of extreme daily temperature and precipitation in the CMIP6 models: Part 2, projections of future change. *Weather Clim Extremes.* 2020;30:100284.
- Wehner M, Reed KA, Li F, Bacmeister J, Chen CT, Paciorek C, Gleckler PJ, Sperber KR, Collins WD, Gettelman A, et al. The effect of horizontal resolution on simulation quality in the community atmospheric model, cam 5.1. *J Adv Model Earth Syst.* 2014;6(4):980–997.
- Westra S, Alexander L, Zwiers F. Global increasing trends in annual maximum daily precipitation. *J Clim.* 2013;26:3904–3918. <https://doi.org/10.1175/JCLI-D-12-00502.1>.
- Westra S, Fowler HJ, Evans JP, Alexander LV, Berg P, Johnson F, Kendon EJ, Lenderink G, Roberts NM. Future changes to the intensity and frequency of short-duration extreme rainfall. *Rev Geophys.* 2014;52(3):522–555. <https://doi.org/10.1002/2014RG000464>.
- van der Wiel K, Kapnick SB, van Oldenborgh GJ, Whan K, Philip S, Vecchi GA, Singh RK, Arrighi J, Cullen H. Rapid attribution of the August 2016 flood-inducing extreme precipitation in south Louisiana to climate change. *Hydrol Earth Syst Sci.* 2017;21(2):897–921. <https://doi.org/10.5194/hess-21-897-2017>.
- Wilby RL, Wigley TML. Future changes in the distribution of daily precipitation totals across North America. *Geophys Res Lett.* 2002;29(7):1135. <https://doi.org/10.1029/2001GL013048>.
- Wing AA, Emanuel KA. Physical mechanisms controlling self-aggregation of convection in idealized numerical modeling simulations. *J Adv Model Earth Syst.* 2014;6(1):59–74.
- Wing AA, Sobel AH, Camargo SJ. Relationship between the potential and actual intensities of tropical cyclones on interannual time scales. *Geophys Res Lett.* 2007;34(8):2007.
- Wolding B, Dias J, Kiladis G, Ahmed F, Powell SW, Maloney E, Branson M. Interactions between moisture and tropical convection. part i: The coevolution of moisture and convection. *J Atmos Sci.* 2020;77(5):1783–1799.
- Wood R, Field PR. The distribution of cloud horizontal sizes. *J Clim.* 2011;24(18):4800–4816. <https://doi.org/10.1175/2011JCLI4056.1>.
- Wuebbles DJ, Meehl G, Hayhoe K, Karl TR, Kunkel K, Santer B, Wehner M, Colle B, Fischer EM, Fu R, Goodman A, Janssen E, Lee H, Li W, Long LN, Olsen S, Sheffield AJ, Sun L. CMIP5, climate model analyses: Climate extremes in the United States. *Bull Amer Meteor Soc.* 2014;95:571–583. <https://doi.org/10.1175/BAMS-D-12-00172.1>.
- Yin J, Guo S, Gentile P, Sullivan SC, Gu L, He S, Chen J, Liu P. Does the hook structure constrain future flood intensification under anthropogenic climate warming. *Water Resour Res.* 57(2). 2021.
- Yu JY, Chou C, Neelin JD. Estimating the gross moist stability of the tropical atmosphere. *J Atmos Sci.* 1998;55:1354–1372.
- Zhang X, Zwiers F, Li G, Wan H, Cannon A. Complexity in estimating past and future extreme short-duration rainfall. *Nat Geosci.* 2017;10:255–259.
- Zhu H, Jiang Z, Li J, Li W, Sun C, Li L. Does CMIP6 inspire more confidence in simulating climate extremes over China? *Adv Atmos Sci.* 2020;37(10):1119–1132.
- Zhu Y, Newell RE. A proposed algorithm for moisture fluxes from atmospheric rivers. *Mon Weather Rev.* 1998;126(3):725–735.

Publisher's Note Springer Nature remains neutral with regard to jurisdictional claims in published maps and institutional affiliations.